

Yukawa coupling corrections to stop, sbottom, and stau production in e^+e^- annihilation

H. Eberl, S. Kraml, W. Majerotto

*Institut für Hochenergiephysik
der Österreichischen Akademie der Wissenschaften,
A-1050 Vienna, Austria*

ABSTRACT: We calculate within the MSSM the one-loop Yukawa coupling corrections to the processes $e^+e^- \rightarrow \tilde{t}_i\tilde{t}_j, \tilde{b}_i\tilde{b}_j, \tilde{\tau}_i\tilde{\tau}_j$ in order of Yukawa coupling squared. These corrections are due to the exchange of charginos, neutralinos, charged and neutral Higgs bosons, and charged and neutral Higgs ghosts. We give the complete analytical formulae. We also perform a detailed numerical analysis of the Yukawa coupling corrections, including also the SUSY-QCD corrections. It turns out that for stop and sbottom production the Yukawa coupling corrections are typically $\sim \pm 10\%$ of the tree-level cross section. For stau production they are about $\pm 5\%$.

Contents

1.Introduction	1
2.Tree–level formulae	2
3.One–loop corrections	3
4.Numerical results and discussion	8
5.Conclusions	10
A.Couplings	10

1. Introduction

Supersymmetry (SUSY) is widely regarded as the most appealing extension of the Standard Model. For testing a specific model of supersymmetry as, for instance, the Minimal Supersymmetric Standard Model (MSSM) [1, 2, 3] precise predictions for the production and decays of SUSY particles are necessary.

Within the last years one–loop SUSY–QCD corrections have been calculated for a variety of processes involving SUSY particles: for $e^+e^- \rightarrow \tilde{q}_i\tilde{q}_j$, ($i, j = 1, 2$) in [4, 5], for $\tilde{q}_i \rightarrow q\tilde{\chi}_k^0$ ($k = 1, \dots, 4$), $\tilde{q}_i \rightarrow q'\tilde{\chi}_l^\pm$ ($l = 1, 2$), in [6], for $\tilde{q}_i \rightarrow q\tilde{g}$ in [7], for $\tilde{q}_2 \rightarrow \tilde{q}_1 Z^0$, $\tilde{q}_i \rightarrow \tilde{q}'_j W^\pm$ in [8], for $\tilde{q}_2 \rightarrow \tilde{q}_1(h^0, H^0, A^0)$, $\tilde{q}_i \rightarrow \tilde{q}'_j H^\pm$ in [9, 10] and for the related Higgs boson decays (h^0, H^0, A^0) $\rightarrow \tilde{q}_i\tilde{q}_j$, $H^\pm \rightarrow \tilde{q}_i\tilde{q}'_j$ in [9, 11], for $qq' \rightarrow \tilde{q}\tilde{q}'$, $gg \rightarrow \tilde{q}\tilde{q}$, $q\bar{q}' \rightarrow \tilde{q}\tilde{q}'$, $gg \rightarrow \tilde{g}\tilde{g}$, $q\bar{q} \rightarrow \tilde{g}\tilde{g}$, $gq \rightarrow \tilde{g}\tilde{q}$ in [12]. Here \tilde{q}_i ($i = 1, 2$) are the mass eigenstates of \tilde{q} , $\tilde{\chi}_k^0$ ($k = 1, \dots, 4$) the neutralinos, $\tilde{\chi}_l^\pm$ ($l = 1, 2$) the charginos, and h^0, H^0, A^0, H^\pm the Higgs bosons of the MSSM.

The SUSY–QCD corrections have turned out to be significant, going up to 90%, depending on the SUSY parameters. The electroweak radiative corrections are expected to be much smaller as $\alpha \ll \alpha_s$, except those which originate from top, bottom and tau Yukawa couplings

$$h_t = \frac{g}{\sqrt{2}m_W} \frac{m_t}{\sin\beta}, \quad h_{b,\tau} = \frac{g}{\sqrt{2}m_W} \frac{m_{b,\tau}}{\cos\beta}. \quad (1.1)$$

They potentially lead to larger corrections due to the large top mass m_t in h_t and/or due to a large coupling $h_{b,\tau}$ in the case of large $\tan\beta$. Such (electroweak) Yukawa

coupling corrections have been calculated for $e^+e^- \rightarrow \tilde{\chi}_i^+ \tilde{\chi}_j^-$ in [13, 14], for $\tilde{b} \rightarrow t\tilde{\chi}_1^-$ in [15], and for $H^+ \rightarrow W^+A^0$ in [16]. The calculations have shown that also these corrections can be important.

In this article we calculate the one-loop Yukawa coupling corrections to the process

$$e^+e^- \rightarrow \tilde{f}_i \tilde{f}_j \quad (i, j = 1, 2), \quad \tilde{f} = \tilde{t}, \tilde{b}, \tilde{\tau}, \quad (1.2)$$

where \tilde{f}_i are the mass eigenstates of \tilde{f} . These corrections are due to the exchange of charginos, neutralinos, Higgs bosons, and Higgs ghosts. They are computed in order $\sim h_{\tilde{f}}^2, h_{\tilde{f}'}^2, h_f h_{f'}$ with $f = t, b, \tau$. f' denotes the isospin partner (e.g. $f = t, f' = b$). We work in the on-shell scheme. The calculation requires the renormalization of the sfermion mixing angle $\theta_{\tilde{f}}$, which was first applied in [5]. In this paper we take a slightly modified renormalization condition for $\theta_{\tilde{f}}$ [15]. In principle, the computation of the Yukawa coupling corrections can be done in the unitary gauge. However, because of electroweak symmetry breaking the longitudinal components of W^\pm and Z^0 exchange behave as the contributions from the Higgs ghosts G^\pm and G^0 , also being proportional to $h_{\tilde{f}}^2, h_{\tilde{f}'}^2, h_f h_{f'}$. This is properly taken into account by using the t'Hooft-Feynman gauge ($\xi = 1$) which we take here. We will see that the contributions due to the exchange of G^0 and G^+ are important.

2. Tree-level formulae

In the case of the 3^{rd} generation the weak eigenstates \tilde{f}_L and \tilde{f}_R mix to mass eigenstates \tilde{f}_1 and \tilde{f}_2 ($m_{\tilde{f}_1} < m_{\tilde{f}_2}$):

$$\tilde{f}_1 = \tilde{f}_L \cos \theta_{\tilde{f}} + \tilde{f}_R \sin \theta_{\tilde{f}} \quad , \quad \tilde{f}_2 = -\tilde{f}_L \sin \theta_{\tilde{f}} + \tilde{f}_R \cos \theta_{\tilde{f}} \quad , \quad (2.1)$$

with the sfermion mixing angle $\theta_{\tilde{f}}$. Using the rotation matrix

$$R^{\tilde{f}} = \begin{pmatrix} \cos \theta_{\tilde{f}} & \sin \theta_{\tilde{f}} \\ -\sin \theta_{\tilde{f}} & \cos \theta_{\tilde{f}} \end{pmatrix} \quad (2.2)$$

we can write eq. (2.1) in the form $\tilde{f}_i = R_{i1}^{\tilde{f}} \tilde{f}_L + R_{i2}^{\tilde{f}} \tilde{f}_R$.

The tree-level production process eq. (1.2) proceeds via γ and Z exchange in the s-channel. The cross section at tree-level is given by:

$$\sigma^0(e^+e^- \rightarrow \tilde{f}_i \tilde{f}_j) = \frac{c_{\tilde{f}}}{3} \frac{\pi \alpha^2}{s} \lambda_{ij}^{3/2} \left[e_f^2 \delta_{ij} - T_{\gamma Z} e_f a_{ij}^{\tilde{f}} \delta_{ij} + T_{ZZ} (a_{ij}^{\tilde{f}})^2 \right] \quad , \quad (2.3)$$

with

$$T_{\gamma Z} = \frac{v_e}{8c_W^2 s_W^2} \frac{s(s - m_Z^2)}{(s - m_Z^2)^2 + \Gamma_Z^2 m_Z^2} \quad , \quad T_{ZZ} = \frac{(a_e^2 + v_e^2)}{256s_W^4 c_W^4} \frac{s^2}{(s - m_Z^2)^2 + \Gamma_Z^2 m_Z^2} \quad . \quad (2.4)$$

Here $\lambda_{ij} = (1 - \mu_i^2 - \mu_j^2)^2 - 4\mu_i^2\mu_j^2$ with $\mu_{i,j}^2 = m_{\tilde{f}_{i,j}}^2/s$. e_f is the charge of the sfermion ($e_t = 2/3, e_b = -1/3, e_\tau = -1$). $c_{\tilde{f}}$ is a color factor, for squarks $c_{\tilde{f}} = 3$ and for sleptons $c_{\tilde{f}} = 1$. v_e and a_e are the vector and axial vector couplings of the electron to the Z boson: $v_e = -1 + 4s_W^2$ (with $s_W \equiv \sin \theta_W$, $c_W \equiv \cos \theta_W$, θ_W is the Weinberg angle), $a_e = -1$, $a_{i,j}^{\tilde{f}}$ are the relevant parts of the couplings to $Z\tilde{f}_i\tilde{f}_j$, see eq. (A.1), and Γ_Z is the total width of the Z boson.

3. One-loop corrections

The corrected cross section including SUSY-QCD corrections in $\mathcal{O}(\alpha_s)$ and Yukawa couplings corrections in $\mathcal{O}(h_f^2, h_{f'}^2, h_f h_{f'})$ [17] can be written as

$$\sigma = \sigma^0 + \Delta\sigma^g + \Delta\sigma^{\tilde{g}} + \Delta\sigma^{yuk}. \quad (3.1)$$

The SUSY-QCD corrections $\Delta\sigma^g$ and $\Delta\sigma^{\tilde{g}}$ are given in [5]. The Yukawa couplings corrections $\Delta\sigma^{yuk}$ can be written as a sum of contributions from exchange of charginos, neutralinos, charged and neutral Higgs particles, and charged and neutral Higgs ghosts, see Fig. 1.

$$\Delta\sigma^{yuk} = \Delta\sigma^{\tilde{\chi}^+} + \Delta\sigma^{\tilde{\chi}^0} + \Delta\sigma^{H^+} + \Delta\sigma^{\mathcal{H}^0} + \Delta\sigma^{G^+} + \Delta\sigma^{G^0}, \quad (3.2)$$

where \mathcal{H}^0 denotes the sum of contributions from neutral Higgs bosons h^0 , H^0 , and A^0 . According to eq. (2.3) the corrections can be written as:

$$\Delta\sigma^x = \frac{c_{\tilde{f}}}{3} \frac{\pi\alpha^2}{s} \lambda_{ij}^{3/2} \left[2e_f \Delta(e_f)_{ij}^{(x)} \delta_{ij} - T_{\gamma Z} (e_f \delta_{ij} \Delta a_{ij}^{(x)} + \Delta(e_f)_{ij}^{(x)} a_{ij}^{\tilde{f}}) + 2T_{ZZ} a_{ij}^{\tilde{f}} \Delta a_{ij}^{(x)} \right], \quad (3.3)$$

(no sum over i, j) where x indicates the exchange of $\tilde{\chi}^+, \tilde{\chi}^0, H^+, \mathcal{H}^0, G^+, G^0$. The terms $\Delta a_{ij}^{(x)}$ and $\Delta(e_f)_{ij}^{(x)}$ are decomposed as:

$$\Delta a_{ij}^{(x)} = \delta a_{ij}^{(v,x)} + \delta a_{ij}^{(w,x)} + \delta a_{ij}^{(\tilde{\theta},x)}, \quad (3.4)$$

$$\Delta(e_f)_{ij}^{(x)} = \delta(e_f)_{ij}^{(v,x)} + \delta(e_f)_{ij}^{(w,x)}. \quad (3.5)$$

The upper index v denotes the vertex corrections (Fig. 1a–f), w the wave-function corrections (Fig. 1g–i), and $\delta a_{ij}^{(\tilde{\theta},x)}$ is the counterterm due to the renormalization of the mixing angle $\theta_{\tilde{f}}$. The latter is necessary because the couplings $a_{ij}^{\tilde{f}}$ explicitly depend on the sfermion mixing angle, see eq. (A.1). The total correction terms $\Delta a_{ij}^{(x)}$ and $\Delta(e_f)_{ij}^{(x)}$ are ultraviolet finite. In the computation we use the one-, two-, and three-point functions A_0, B_0, C_0, C_1 , and C_2 [18] in the convention of [19].

First we calculate the vertex corrections corresponding to Fig. 1a–f. We introduce the variable A_V^x which is connected to the vertex correction terms $\delta a_{ij}^{(v,x)}$, eq. (3.4),

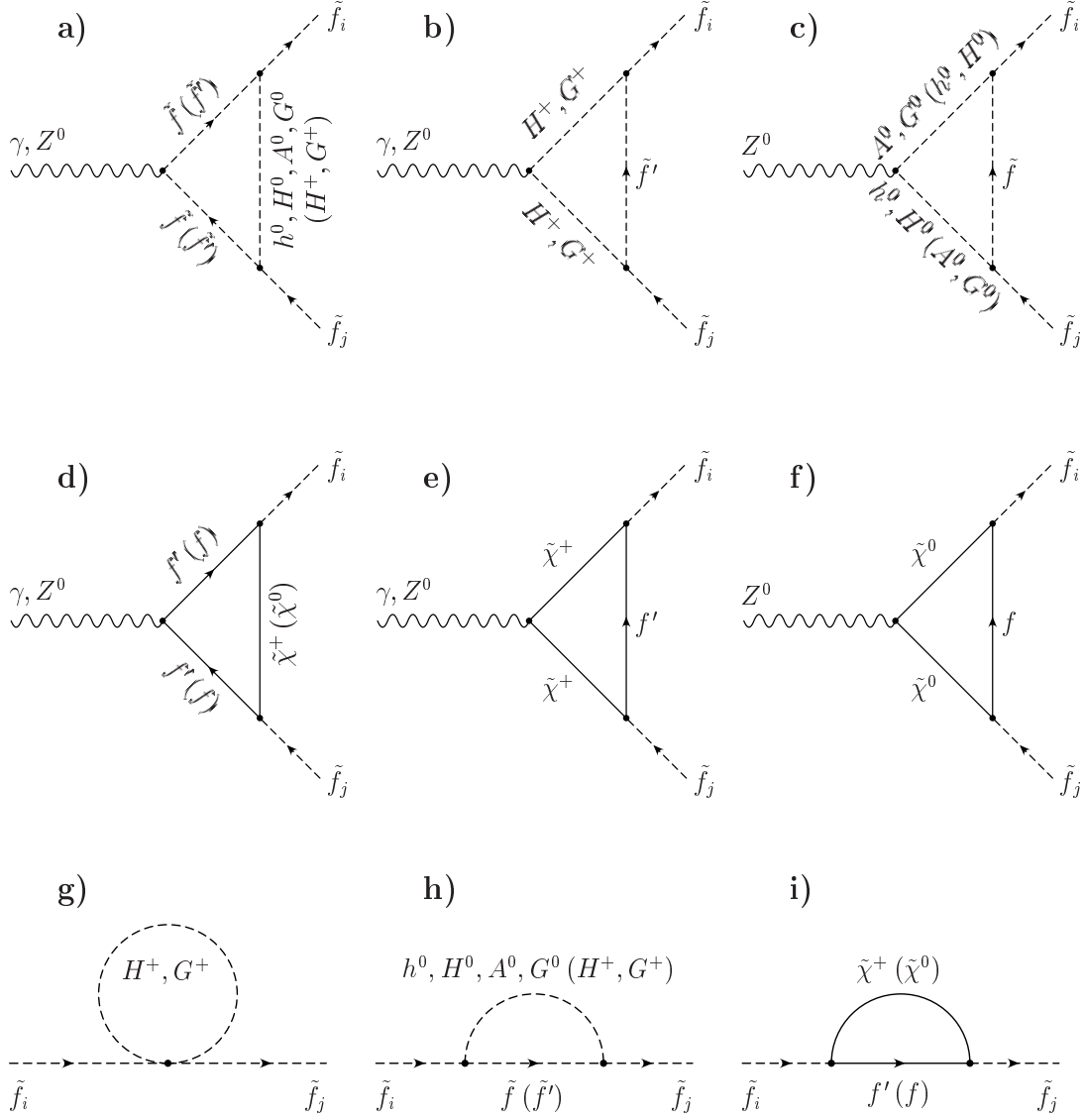


Figure 1: Feynman diagrams for the one-loop corrections to $e^+e^- \rightarrow \tilde{f}_i\tilde{f}_j$ in order of Yukawa couplings squared.

and $\delta(e_f)_{ij}^{(v,x)}$, eq. (3.5), by the relations

$$\delta a_{ij}^{(v,x)} = \frac{1}{(4\pi)^2} A_Z^x, \quad \delta(e_f)_{ij}^{(v,x)} = \frac{1}{(4\pi)^2} A_\gamma^x. \quad (3.6)$$

For the one-loop graphs of $(Z^{0*}, \gamma^*) \rightarrow \tilde{f}_i\tilde{f}_j$ with three scalars propagating in the loop, Fig. 1a–c, i. e. the graphs with $h^0, H^0, A^0, H^\pm, G^0$, and G^\pm exchange, one

has the following generic formula

$$A = g_0 g_1 g_2 (C_0 + C_1 + C_2) \quad (3.7)$$

with $(m_{\tilde{f}_i}^2, s, m_{\tilde{f}_j}^2, M_0^2, M_1^2, M_2^2)$ as the arguments of the C–functions. The couplings g_0, g_1, g_2 and the masses M_0, M_1, M_2 of the particles in the loop can be read off from Table 1. The contributions from the ghosts G^+ and G^0 are not given explicitly because they can be easily calculated from the contributions with H^+ and A^0 by using the transformation rules

$$\beta \rightarrow \beta - \frac{\pi}{2}, \quad m_{H^+} \rightarrow m_{W^+}, \quad m_{A^0} \rightarrow m_{Z^0}. \quad (3.8)$$

name of coeff.	M_0	M_1	M_2	$V = Z$ g_0	$V = \gamma$ g_0	g_1	g_2	sum over indices
$A_V^{H_k^0}$	$m_{H_k^0}$	$m_{\tilde{f}_l}$	$m_{\tilde{f}_m}$	$-2a_{lm}^{\tilde{f}}$	$-2e_f \delta_{lm}$	$h_f(G_{\tilde{f},k})_{il}$	$h_f(G_{\tilde{f},k})_{mj}$	$k = 1, 2, 3$ $l, m = 1, 2$
$A_V^{H^+}$	m_{H^+}	$m_{\tilde{f}'_l}$	$m_{\tilde{f}'_m}$	$-a_{lm}^{\tilde{f}'}$	$-e_{f'} \delta_{lm}$	$(G_{\tilde{f}'})_{il}$	$(G_{\tilde{f}'})_{jm}$	$l, m = 1, 2$
$A_V^{A^0 H_k^0}$	$m_{\tilde{f}_l}$	m_{A^0}	$m_{H_k^0}$	$-4f_k(\alpha - \beta)$	0	$ih_f(G_{\tilde{f},3})_{il}$	$h_f(G_{\tilde{f},k})_{lj}$	$k, l = 1, 2$
$A_V^{H_k^0 A^0}$	$m_{\tilde{f}_l}$	$m_{H_k^0}$	m_{A^0}	$4f_k(\alpha - \beta)$	0	$h_f(G_{\tilde{f},k})_{il}$	$ih_f(G_{\tilde{f},3})_{lj}$	$k, l = 1, 2$
$A_V^{H^+ H^-}$	$m_{\tilde{f}'_l}$	m_{H^+}	m_{H^+}	$-2 \cos 2\theta_W$	-1	$(G_{\tilde{f}'})_{il}$	$(G_{\tilde{f}'})_{jl}$	$l = 1, 2$

Table 1: Parameters for calculating the coefficients A , with three scalar particles in the loop, eq. (3.6). See also eq. (3.7) and Fig. 1a–c. We used $H_k^0 \equiv \{h^0, H^0, A^0\}$ and $f_1 \equiv \cos$ and $f_2 \equiv \sin$.

For the one–loop graphs of $(Z^{0*}, \gamma^*) \rightarrow \tilde{f}_i \tilde{f}_j$ with a closed fermion loop, Fig. 1d–f, i. e. the graphs with $\tilde{\chi}^\pm$ and $\tilde{\chi}^0$ exchange, one has the following generic formula:

$$\begin{aligned}
A = & M_0 M_2 (g_0^L g_1^L g_2^L + g_0^R g_1^R g_2^R)(C_0 + C_1 + C_2) \\
& + M_0 M_1 (g_0^L g_1^R g_2^R + g_0^R g_1^L g_2^L)(C_0 + C_1 + C_2) \\
& + M_1 M_2 (g_0^L g_1^R g_2^L + g_0^R g_1^L g_2^R)(C_1 + C_2) \\
& + (g_0^L g_1^L g_2^R + g_0^R g_1^R g_2^L)(B_0(s, M_1^2, M_2^2) \\
& \quad + M_0^2(2C_0 + C_1 + C_2) + m_{\tilde{f}_i}^2 C_1 + m_{\tilde{f}_j}^2 C_2). \quad (3.9)
\end{aligned}$$

Here the set of arguments for the C–functions is $(m_{\tilde{f}_i}^2, s, m_{\tilde{f}_j}^2, M_0^2, M_1^2, M_2^2)$. The couplings $g_{0,1,2}^L$ and $g_{0,1,2}^R$ as well as the masses M_0, M_1, M_2 of the particles in the loop are given in Table 2.

name of coeff.	M_0	M_1	M_2	$V = Z$		$V = \gamma$ $g_0^R = g_0^L$	g_1^R	g_1^L	g_2^R	g_2^L	sum over indices
				g_0^R	g_0^L						
$A_V^{\tilde{\chi}^+}$	$m_{\tilde{\chi}_l^+}$	$m_{f'}$	$m_{f'}$	$4 C_R^{f'}$	$4 C_L^{f'}$	$e_{f'}$	$k_{il}^{\tilde{f}}$	$l_{il}^{\tilde{f}}$	$l_{jl}^{\tilde{f}}$	$k_{jl}^{\tilde{f}}$	$l = 1, 2$
$A_V^{\tilde{\chi}^0}$	$m_{\tilde{\chi}_l^0}$	m_f	m_f	$4 C_R^f$	$4 C_L^f$	e_f	$\hat{b}_{il}^{\tilde{f}}$	$\hat{a}_{il}^{\tilde{f}}$	$\hat{a}_{jl}^{\tilde{f}}$	$\hat{b}_{jl}^{\tilde{f}}$	$l = 1, \dots, 4$
$A_V^{\tilde{\chi}^+ \tilde{\chi}^-}(\tilde{t})$	m_b	$m_{\tilde{\chi}_k^+}$	$m_{\tilde{\chi}_l^+}$	$-4 O_{kl}^{\prime R}$	$-4 O_{kl}^{\prime L}$	δ_{kl}	$k_{ik}^{\tilde{t}}$	$l_{ik}^{\tilde{t}}$	$l_{jl}^{\tilde{t}}$	$k_{jl}^{\tilde{t}}$	$k, l = 1, 2$
$A_V^{\tilde{\chi}^+ \tilde{\chi}^-}(\tilde{b})$	m_t	$m_{\tilde{\chi}_k^+}$	$m_{\tilde{\chi}_l^+}$	$4 O_{kl}^{\prime L}$	$4 O_{kl}^{\prime R}$	$-\delta_{kl}$	$k_{ik}^{\tilde{b}}$	$l_{ik}^{\tilde{b}}$	$l_{jl}^{\tilde{b}}$	$k_{jl}^{\tilde{b}}$	$k, l = 1, 2$
$A_V^{\tilde{\chi}^0 \tilde{\chi}^0}$	m_f	$m_{\tilde{\chi}_k^0}$	$m_{\tilde{\chi}_l^0}$	$4 O_{kl}^{\prime\prime L}$	$-4 O_{kl}^{\prime\prime L}$	0	$\hat{b}_{ik}^{\tilde{f}}$	$\hat{a}_{ik}^{\tilde{f}}$	$\hat{a}_{jl}^{\tilde{f}}$	$\hat{b}_{jl}^{\tilde{f}}$	$k, l = 1, \dots, 4$

Table 2: Parameters for calculating the coefficients A with a closed fermion loop, eq. (3.6). See also eq. (3.9) and Fig. 1d–f. The coefficient $A_V^{\tilde{\chi}^+ \tilde{\chi}^-}(\tilde{\tau})$ is obtained from $A_V^{\tilde{\chi}^+ \tilde{\chi}^-}(\tilde{b})$ by using the rules $t \rightarrow \nu_\tau$ and $b \rightarrow \tau$. Further we used $O^{\prime\prime R} = -O^{\prime\prime L}$.

The sfermion wave–function renormalization due to the sfermion self–energy graphs (Fig. 1g–i) with exchange of the particle(s) x leads in the on–shell scheme to

$$\delta a_{ij}^{(w,x)} = \frac{1}{2}(\delta Z_{ii}^{(x)} + \delta Z_{jj}^{(x)})a_{ij}^{\tilde{f}} + \delta Z_{i'i}^{(x)}a_{i'j}^{\tilde{f}} + \delta Z_{j'j}^{(x)}a_{ij'}^{\tilde{f}}, \quad (3.10)$$

$$\delta a_{ij}^{(w,x)} = \frac{1}{2}(\delta Z_{ii}^{(x)} + \delta Z_{jj}^{(x)})a_{ij}^{\tilde{f}} + \delta Z_{i'i}^{(x)}a_{i'j}^{\tilde{f}} + \delta Z_{j'j}^{(x)}a_{ij'}^{\tilde{f}}, \quad (3.11)$$

$$\delta(e_f)_{ii}^{(w,x)} = e_f \delta Z_{ii}^{(x)}, \quad \delta(e_f)_{12}^{(w,x)} = \frac{e_f}{m_{\tilde{f}_1}^2 - m_{\tilde{f}_2}^2} \left\{ \delta Z_{12}^{(x)} + \delta Z_{21}^{(x)} \right\}, \quad (3.12)$$

with $i \neq i', j \neq j'$, $\delta Z_{ii}^{(x)} = -\text{Re} \left\{ \Sigma_{ii}^{\prime(x)}(m_{\tilde{f}_i}^2) \right\}$, where $\Sigma_{ii}^{\prime(x)}(m^2) = \partial \Sigma_{ii}^{(x)}(k^2) / \partial k^2 |_{k^2=m^2}$, and

$$\delta Z_{12}^{(x)} = \frac{\Sigma_{12}^{(x)}(m_{\tilde{f}_2}^2)}{m_{\tilde{f}_1}^2 - m_{\tilde{f}_2}^2}, \quad \text{and} \quad \delta Z_{21}^{(x)} = -\frac{\Sigma_{12}^{(x)}(m_{\tilde{f}_1}^2)}{m_{\tilde{f}_1}^2 - m_{\tilde{f}_2}^2}. \quad (3.13)$$

Note, that $\Sigma_{12}(k^2) = \Sigma_{21}(k^2)$.

The self–energy corresponding to Fig. 1g is

$$\Sigma_{ij}^{(H^+)} = -\frac{1}{(4\pi)^2} (b_f R_{i1}^{\tilde{f}} R_{j1}^{\tilde{f}} + c_f R_{i2}^{\tilde{f}} R_{j2}^{\tilde{f}}) A_0(m_{H^+}^2), \quad (3.14)$$

with $b_u = c_d = h_d^2 \sin^2 \beta$ and $b_d = c_u = h_u^2 \cos^2 \beta$ where $(u, d) \equiv (t, b)$ or (ν_τ, τ) . The indices i and j refer to the sfermions \tilde{f}_i and \tilde{f}_j . $R^{\tilde{f}}$ is given in eq. (2.2).

Next we treat the self–energies corresponding to Fig. 1h. The results for the graphs with the neutral Higgs particles h^0 , H^0 , and A^0 and a sfermion in the loop are

$$\Sigma_{ij}^{(H_k^0 \tilde{f})}(k^2) = \frac{2h_f^2}{(4\pi)^2} \sum_{l=1,2} (G_{\tilde{f},k})_{li} (G_{\tilde{f},k})_{jl} B_0(k^2, m_{H_k^0}^2, m_{\tilde{f}_l}^2). \quad (3.15)$$

The couplings $G_{\tilde{f},k}$ are given in eqs. (A.4) – (A.9). Note that for $k = 1, 2$ the matrices $(G_{\tilde{f},k})$ are symmetric, therefore $(G_{\tilde{f},k})_{li} = (G_{\tilde{f},k})_{il}$. For the case of A^0 exchange the matrix $(G_{\tilde{f},k})$ is totally antisymmetric, $(G_{\tilde{f},3})_{li} = -(G_{\tilde{f},3})_{il}$.

Analogously we get for the graphs with a charged Higgs particle and a sfermion in the loop,

$$\Sigma_{ij}^{(H^+\tilde{f}')} (k^2) = \frac{1}{(4\pi)^2} \sum_{l=1,2} (G_{\tilde{f}\tilde{f}'}^l)_{il} (G_{\tilde{f}\tilde{f}'}^l)_{jl} B_0(k^2, m_{H^+}^2, m_{\tilde{f}'}^2), \quad (3.16)$$

with the couplings $G_{\tilde{f}\tilde{f}'}$ given in eqs. (A.10) and (A.11).

The ghost contributions $\Sigma_{ij}^{(G^+)}$, $\Sigma_{ij}^{(G^0\tilde{f})}$, and $\Sigma_{ij}^{(G^+\tilde{f}'')}$ can be calculated from $\Sigma_{ij}^{(H^+)}$, $\Sigma_{ij}^{(H^0\tilde{f})}$, and $\Sigma_{ij}^{(H^+\tilde{f}'')}$, respectively, using eq. (3.8).

As to the self-energies corresponding to Fig. 1i, for chargino exchange we get

$$\begin{aligned} \Sigma_{ij}^{(\tilde{\chi}^+)} (k^2) = & -\frac{1}{(4\pi)^2} \sum_{l=1,2} \left[2m_{f'} m_l (l_{il}^{\tilde{f}} k_{jl}^{\tilde{f}} + k_{il}^{\tilde{f}} l_{jl}^{\tilde{f}}) B_0(k^2, m_l^2, m_{f'}^2) \right. \\ & \left. + (l_{il}^{\tilde{f}} l_{jl}^{\tilde{f}} + k_{il}^{\tilde{f}} k_{jl}^{\tilde{f}}) \left(A_0(m_l^2) + A_0(m_{f'}^2) + (m_l^2 + m_{f'}^2 - k^2) B_0(k^2, m_l^2, m_{f'}^2) \right) \right], \end{aligned} \quad (3.17)$$

where the index l refers to the charginos $\tilde{\chi}_l^+$ (with $m_l \equiv m_{\tilde{\chi}_l^+}$). For neutralino exchange we get

$$\begin{aligned} \Sigma_{ij}^{(\tilde{\chi}^0)} (k^2) = & -\frac{1}{(4\pi)^2} \sum_{k=1}^4 \left[2m_f m_k (\hat{a}_{ik}^{\tilde{f}} \hat{b}_{jk}^{\tilde{f}} + \hat{b}_{ik}^{\tilde{f}} \hat{a}_{jk}^{\tilde{f}}) B_0(k^2, m_k^2, m_f^2) \right. \\ & \left. + (\hat{a}_{ik}^{\tilde{f}} \hat{a}_{jk}^{\tilde{f}} + \hat{b}_{ik}^{\tilde{f}} \hat{b}_{jk}^{\tilde{f}}) \left(A_0(m_k^2) + A_0(m_f^2) + (m_k^2 + m_f^2 - k^2) B_0(k^2, m_k^2, m_f^2) \right) \right], \end{aligned} \quad (3.18)$$

where the index k refers to the neutralinos $\tilde{\chi}_k^0$ (with $m_k \equiv m_{\tilde{\chi}_k^0}$).

For the renormalization of the sfermion mixing angle $\theta_{\tilde{f}}$ we get from eq. (A.1)

$$\delta a_{ij}^{(\tilde{\theta},x)} = \begin{pmatrix} 2a_{12}^{\tilde{f}} & a_{22}^{\tilde{f}} - a_{11}^{\tilde{f}} \\ a_{22}^{\tilde{f}} - a_{11}^{\tilde{f}} & -2a_{12}^{\tilde{f}} \end{pmatrix} \delta\theta_{\tilde{f}}^{(x)}. \quad (3.19)$$

We require a process independent renormalization condition for $\theta_{\tilde{f}}$ that involves both mass eigenstates \tilde{f}_1 and \tilde{f}_2 (see also [15]),

$$\delta\theta_{\tilde{f}}^{(x)} = \frac{1}{2} (\delta Z_{12}^{(x)} - \delta Z_{21}^{(x)}) = \frac{\Sigma_{12}^{(x)}(m_{\tilde{f}_1}^2) + \Sigma_{12}^{(x)}(m_{\tilde{f}_2}^2)}{2(m_{\tilde{f}_1}^2 - m_{\tilde{f}_2}^2)}. \quad (3.20)$$

We want to point out that in the case of chargino exchange this antisymmetric combination of δZ_{12} and δZ_{21} is the only possible fixing condition for $\delta\theta_{\tilde{f}}^{(\tilde{\chi}^+)}$ as a function of the off-diagonal self-energies.

4. Numerical results and discussion

Let us now turn to the numerical analysis. As input parameters we take the MSSM parameters $M_{\tilde{Q},\tilde{U},\tilde{D},\tilde{L},\tilde{E}}, A_{t,b,\tau}, m_A, \mu, M$, and $\tan\beta$. M is the SU(2) gaugino mass; for the U(1) gaugino mass M' and the gluino mass $m_{\tilde{g}}$ we assume the GUT relations $M' = (5/3)\tan^2\theta_W M$ and $m_{\tilde{g}} = (\alpha_s(m_{\tilde{g}})/\alpha_2)M$. Moreover, we take $m_t = 175$ GeV, $m_b = 5$ GeV, $m_Z = 91.187$ GeV, $\sin^2\theta_W = 0.232$, $m_W = m_Z \cos\theta_W$, $\alpha(m_Z) = 1/128.87$, and $\alpha_s(m_Z) = 0.12$ [with $\alpha_s(Q) = 12\pi/((33 - 2n_f)\ln(Q^2/\Lambda_{n_f}^2))$, n_f being the number of quark flavours]. For the radiative corrections to the h^0 and H^0 masses and their mixing angle α ($-\frac{\pi}{2} \leq \alpha < \frac{\pi}{2}$ by convention) we use the formulae of [22]; for those to m_{H^\pm} we follow [23] *. In order to respect the experimental mass bounds from LEP2 [24] and Tevatron [25] we impose $m_{h^0} > 90$ GeV, $m_{\tilde{\chi}_1^\pm} > 95$ GeV, $m_{\tilde{t}_1,\tilde{b}_1,\tilde{\tau}_1} > 85$ GeV, and $m_{\tilde{g}} > 200$ GeV. Moreover, we require $\delta\rho(\tilde{t} - \tilde{b}) < 0.0012$ [26] from electroweak precision measurements using the one-loop formulae of [27] and $A_t^2 < 3(M_{\tilde{Q}}^2 + M_{\tilde{U}}^2 + m_{H_2}^2)$, $A_{b,\tau}^2 < 3(M_{\tilde{Q},\tilde{L}}^2 + M_{\tilde{D},\tilde{E}}^2 + m_{H_1}^2)$ with $m_{H_2}^2 = (m_A^2 + m_Z^2)\cos^2\beta - \frac{1}{2}m_Z^2$ and $m_{H_1}^2 = (m_A^2 + m_Z^2)\sin^2\beta - \frac{1}{2}m_Z^2$ [28] to guarantee tree-level vacuum stability.

For stop and sbottom production we choose $M_{\tilde{Q}} = 225$ GeV, $M_{\tilde{U}} = 200$ GeV, $M_{\tilde{D}} = 250$ GeV, $A_t = A_b = 400$ GeV, $m_A = 300$ GeV, and $\tan\beta = 4$ as an illustrative parameter point. Moreover, we consider two sets of M and μ values: a “gaugino scenario” with $M = 200$ GeV and $\mu = 1000$ GeV and a “higgsino scenario” with $M = 1000$ GeV and $\mu = 200$ GeV. The corresponding physical masses and mixing angles are listed in Tables 3 and 4.

We first discuss the gaugino scenario of Table 3: Figure 2 shows the 1-loop (SUSY-QCD [5] and Yukawa coupling) corrected cross sections of $e^+e^- \rightarrow \tilde{t}_i\tilde{t}_j$ and $e^+e^- \rightarrow \tilde{b}_i\tilde{b}_j$ and the tree-level cross sections as a function of \sqrt{s} . As can be seen, the radiative corrections can have sizable effects. We now study the relative importance of the various contributions to these corrections. In Fig. 3 a we show the \sqrt{s} dependence of the gluon, gluino, and Yukawa coupling corrections to $\sigma(e^+e^- \rightarrow \tilde{t}_1\tilde{t}_1)$ relative to the tree-level cross section. The gluon correction is always positive and approaches 10% of σ^0 for high \sqrt{s} . In contrast to that the gluino and the Yukawa coupling corrections can have either sign. In this example $|\Delta\sigma^{\tilde{g}}/\sigma^0| \lesssim 4\%$; $|\Delta\sigma^{yuk}/\sigma^0|$ can go up to 6%. The various contributions to the Yukawa coupling corrections are disentangled in Fig. 3 b, where we plot $\Delta\sigma^x/\sigma^0$ with $x = \tilde{\chi}^+, \tilde{\chi}^0, \mathcal{H}^0, H^+, G$, see Eq. (3.2) and $\Delta\sigma^G = \Delta\sigma^{G^+} + \Delta\sigma^{G^0}$. For $\sqrt{s} \lesssim 830$ GeV all contributions are positive with those from Higgs exchange being the most important ones. For larger \sqrt{s} , $\Delta\sigma^{\mathcal{H}^0}$ and $\Delta\sigma^{H^+}$ become negative. Together, they can be up to -60% of the gluon correction. This comes from the large value of μ ($\mu = 1000$ GeV) which directly enters the $\tilde{q}\tilde{q}H$ couplings. For $\sqrt{s} \sim 2$ TeV the correction due to chargino exchange

* Notice that [22, 23] have the opposite sign convention for the parameter μ .

also becomes important because $\tilde{\chi}_2^+ = \tilde{H}^+$ with a mass of ~ 1 TeV. Analogously, Figs. 4 a and 4 b show $\Delta\sigma/\sigma^0$ and $\Delta\sigma^x/\sigma^0$ ($x = \tilde{\chi}^+, \tilde{\chi}^0, \mathcal{H}^0, H^+, G$) for $\tilde{t}_1\tilde{t}_2 + \text{c.c.}$ production for the gaugino scenario (Table 3). In this case the Yukawa coupling correction is even more important than in Fig. 3. Together with the gluino correction it can even cancel the gluon correction. The reason is that for $900 \text{ GeV} \lesssim \sqrt{s} \lesssim 2000 \text{ GeV}$ all relevant Yukawa coupling contributions are negative. Again there is a large correction due to neutral Higgs boson exchange. The correction due to chargino exchange is sizable for $\sqrt{s} \sim 2\mu$. Notice also that here the neutralino contribution plays an important rôle.

As for sbottom production, we see in Fig. 5 a that Yukawa coupling corrections can be important, too, even for small $\tan\beta$: $\Delta\sigma^{yuk}$ reaches -17% of σ^0 . This is due to the top Yukawa coupling which enters the $t\tilde{b}\tilde{\chi}^\pm$ and the $\tilde{t}\tilde{b}H^\pm$ couplings. Indeed, $\Delta\sigma^{H^+}$ and for $\sqrt{s} \sim 2\mu$ also $\Delta\sigma^{\tilde{\chi}^+}$ give the main contributions to $\Delta\sigma^{yuk}$ as can be seen in Fig. 5 b. However, for $\sqrt{s} \gtrsim 1700 \text{ GeV}$ the Yukawa coupling correction is less important than the gluino correction because $\Delta\sigma^{H^+}$ and $\Delta\sigma^{\tilde{\chi}^+}$ are of similar size but of opposite sign.

Let us now turn to the higgsino scenario of Table 4. Figure 6 shows the relative corrections to the cross section of $e^+e^- \rightarrow \tilde{t}_1\tilde{t}_1$ for this scenario as a function of \sqrt{s} . Again Yukawa coupling corrections turn out to be important. In this case (small μ), however, the dominant contributions come from exchanges of the lighter chargino and neutralinos. Higgs and ghost contributions are negligible. Notice the spikes at $\sqrt{s} \sim 400 \text{ GeV}$. In Fig. 7 we show the corrections to the cross section of $\tilde{b}_1\tilde{b}_1$ production for the higgsino scenario. While the gluino correction is $\lesssim 0.01 \sigma^0$ the Yukawa coupling correction is about $0.04 \sigma^0$ for $\sqrt{s} \gtrsim 800 \text{ GeV}$. For $\sqrt{s} \lesssim 800 \text{ GeV}$ the contributions from H^+ , G^+ , and $\tilde{\chi}^+$ are of comparable size; for larger \sqrt{s} the chargino contribution clearly dominates.

We finally discuss the Yukawa coupling correction to the stau production cross section. This correction may be important for large $\tan\beta$ (large τ Yukawa coupling). It turns out that in this case $\Delta\sigma^{yuk}(e^+e^- \rightarrow \tilde{\tau}_i\tilde{\tau}_j)$ is typically up to $\pm 5\%$ of the tree-level cross section. As an example, we plot in Fig. 8 the \sqrt{s} dependence of the relevant Yukawa coupling correction contributions and the total correction of $\sigma(e^+e^- \rightarrow \tilde{\tau}_i\tilde{\tau}_i)$, $i = 1, 2$, for $M_{\tilde{L}} = 280 \text{ GeV}$, $M_{\tilde{E}} = 250 \text{ GeV}$, $A_\tau = 100 \text{ GeV}$, $M = 200 \text{ GeV}$, $\mu = 1000 \text{ GeV}$, $\tan\beta = 30$, and $m_A = 300 \text{ GeV}$. This leads to $m_{\tilde{\tau}_1} = 137 \text{ GeV}$, $m_{\tilde{\tau}_2} = 355 \text{ GeV}$, and $\cos\theta_{\tilde{\tau}} = 0.65$. For the squark parameters, which are needed for the radiative corrections to the Higgs masses, we have taken $M_{\tilde{Q}} = M_{\tilde{U}} = M_{\tilde{D}} = 500 \text{ GeV}$, and $A_t = A_b = 300 \text{ GeV}$. In both Figs. 8 a and 8 b Higgs boson and ghost exchanges yield the most important contributions because their couplings to staus directly involve the parameter μ . For $M = 1000 \text{ GeV}$, $\mu = 200 \text{ GeV}$, and the other parameters as above, we get $m_{\tilde{\tau}_1} = 243 \text{ GeV}$, $m_{\tilde{\tau}_2} = 293 \text{ GeV}$, and $\cos\theta_{\tilde{\tau}} = 0.64$. The Yukawa coupling correction again changes the tree-

level cross section by $\lesssim \pm 5\%$ with the dominant contributions coming from chargino and neutralino loops. Higgs and ghost contributions are of minor importance in this case.

5. Conclusions

We have calculated the supersymmetric Yukawa coupling corrections to stop, sbottom, and stau production in e^+e^- annihilation. We have evaluated these corrections numerically for two scenarios, a gaugino scenario ($M \ll |\mu|$) and a higgsino scenario ($|\mu| \ll M$). It turns out that for stop and sbottom production the Yukawa coupling correction is typically $\pm 5\%$ to $\pm 10\%$ of the tree-level cross section. It can thus be as large as the SUSY-QCD correction. In the case of stau production the Yukawa coupling correction can also change the tree-level cross section by $\mathcal{O}(\pm 5\%)$. In the case $M \sim |\mu|$, where the individual charginos and neutralinos have both sizable gaugino and higgsino components, it may be that in addition to the graphs considered, also box graphs contribute. Because of the complexity of their computation, their influence will be studied in a separate article.

In conclusion, we have shown that the corrections due to the Yukawa couplings are relevant for precision measurements at a future e^+e^- Linear Collider.

Acknowledgments

We thank M. Diaz for valuable contributions in the first stage of this work. We also thank W. Porod and A. Bartl for discussions. This work was supported by the ‘‘Fonds zur F6orderung der wissenschaftlichen Forschung’’ of Austria, project no. P13139-PHY.

A. Couplings

In this section we give the couplings which are necessary for calculating the matrix elements corresponding to the graphs of Fig. 1. The $Z^0 \tilde{f}_i^* \tilde{f}_j$ coupling is proportional to $g/(4 \cos \theta_W) a_{ij}^{\tilde{f}}$ with

$$a_{ij}^{\tilde{f}} = \begin{pmatrix} 4(I_f^{3L} \cos^2 \theta_{\tilde{f}} - e_f s_W^2) & -2I_f^{3L} \sin 2\theta_{\tilde{f}} \\ -2I_f^{3L} \sin 2\theta_{\tilde{f}} & 4(I_f^{3L} \sin^2 \theta_{\tilde{f}} - e_f s_W^2) \end{pmatrix}. \quad (\text{A.1})$$

With the abbreviation

$$C_{L,R}^f = I_f^{3L,R} - s_W^2 e_f. \quad (\text{A.2})$$

$a_{ij}^{\tilde{f}}$ can also be written as

$$\frac{a_{ij}^{\tilde{f}}}{4} = R^{\tilde{f}} \begin{pmatrix} C_L^f & 0 \\ 0 & C_R^f \end{pmatrix} (R^{\tilde{f}})^T = R^{\tilde{f}} \begin{pmatrix} I_f^{3L} & 0 \\ 0 & 0 \end{pmatrix} (R^{\tilde{f}})^T - e_f s_W^2 \begin{pmatrix} 1 & 0 \\ 0 & 1 \end{pmatrix}. \quad (\text{A.3})$$

Here $I_f^{3L} = 1/2(-1/2)$ for up-type (down-type) fermions f and $I_f^{3R} = 0$ for all fermions. The matrix $R^{\tilde{f}}$ is given in eq. (2.2).

The Higgs–sfermion–sfermion couplings are given in $O(h_t, h_b, h_\tau)$. The Yukawa couplings h_t, h_b , and h_τ are already given in eq. (1.1). The couplings for the $\mathcal{H}^0 \tilde{f}_i^* \tilde{f}_j$ interactions ($\mathcal{H}^0 \equiv \{h^0, H^0, A^0\}$, $i, j = 1, 2$) are $-i\sqrt{2}h_f(G_{\tilde{f},k})_{ij}$ with

$$G_{\tilde{t},1} = R^{\tilde{t}} \cdot \begin{pmatrix} m_t \cos \alpha & \frac{1}{2}(A_t \cos \alpha + \mu \sin \alpha) \\ \frac{1}{2}(A_t \cos \alpha + \mu \sin \alpha) & m_t \cos \alpha \end{pmatrix} \cdot (R^{\tilde{t}})^T, \quad (\text{A.4})$$

$$G_{\tilde{d},1} = -R^{\tilde{d}} \cdot \begin{pmatrix} m_d \sin \alpha & \frac{1}{2}(A_d \sin \alpha + \mu \cos \alpha) \\ \frac{1}{2}(A_d \sin \alpha + \mu \cos \alpha) & m_d \sin \alpha \end{pmatrix} \cdot (R^{\tilde{d}})^T, \quad (\text{A.5})$$

$$G_{\tilde{t},2} = R^{\tilde{t}} \cdot \begin{pmatrix} m_t \sin \alpha & \frac{1}{2}(A_t \sin \alpha - \mu \cos \alpha) \\ \frac{1}{2}(A_t \sin \alpha - \mu \cos \alpha) & m_t \sin \alpha \end{pmatrix} \cdot (R^{\tilde{t}})^T, \quad (\text{A.6})$$

$$G_{\tilde{d},2} = R^{\tilde{d}} \cdot \begin{pmatrix} m_d \cos \alpha & \frac{1}{2}(A_d \cos \alpha - \mu \sin \alpha) \\ \frac{1}{2}(A_d \cos \alpha - \mu \sin \alpha) & m_d \cos \alpha \end{pmatrix} \cdot (R^{\tilde{d}})^T, \quad (\text{A.7})$$

$$G_{\tilde{t},3} = \begin{pmatrix} 0 & -\frac{i}{2}(A_t \cos \beta + \mu \sin \beta) \\ \frac{i}{2}(A_t \cos \beta + \mu \sin \beta) & 0 \end{pmatrix}, \quad (\text{A.8})$$

$$G_{\tilde{d},3} = \begin{pmatrix} 0 & -\frac{i}{2}(A_d \sin \beta + \mu \cos \beta) \\ \frac{i}{2}(A_d \sin \beta + \mu \cos \beta) & 0 \end{pmatrix}. \quad (\text{A.9})$$

Here \tilde{d} stands for \tilde{b} or $\tilde{\tau}$. The couplings for the $H^\pm \tilde{f}_i^* \tilde{f}'_j$ interactions are $i(G_{\tilde{f}\tilde{f}'})_{ij}$ with

$$G_{\tilde{t}\tilde{b}} = R^{\tilde{t}} \cdot \begin{pmatrix} h_b m_b \sin \beta + h_t m_t \cos \beta & h_b (A_b \sin \beta + \mu \cos \beta) \\ h_t (A_t \cos \beta + \mu \sin \beta) & \frac{1}{2} \left(h_t \frac{m_b}{\cos \beta} + h_b \frac{m_t}{\sin \beta} \right) \end{pmatrix} \cdot (R^{\tilde{b}})^T, \quad (\text{A.10})$$

and

$$G_{\tilde{\tau}\tilde{\nu}_\tau} = h_\tau \begin{pmatrix} m_\tau \sin \beta \cos \theta_{\tilde{\tau}} + (A_\tau \sin \beta + \mu \cos \beta) \sin \theta_{\tilde{\tau}} & 0 \\ -m_\tau \sin \beta \sin \theta_{\tilde{\tau}} + (A_\tau \sin \beta + \mu \cos \beta) \cos \theta_{\tilde{\tau}} & 0 \end{pmatrix}. \quad (\text{A.11})$$

Note that $(G_{\tilde{f}\tilde{f}'})_{ij} = (G_{\tilde{f}'\tilde{f}})_{ji}$.

For the interaction of Z^0 with charginos we need

$$\begin{aligned} O'_{ij}{}^L &= -V_{i1}V_{j1} - \frac{1}{2}V_{i2}V_{j2} + \delta_{ij}s_W^2, \\ O'_{ij}{}^R &= -U_{i1}U_{j1} - \frac{1}{2}U_{i2}U_{j2} + \delta_{ij}s_W^2, \end{aligned} \quad (\text{A.12})$$

with the real rotation matrices U and V which diagonalize the chargino mass matrix [2, 20], ($i, j = 1, 2$). For the interaction of Z^0 with neutralinos we need

$$O''_{kl}{}^L = -O''_{kl}{}^R = \frac{1}{2} \left((-N_{k3}N_{l3} + N_{k4}N_{l4}) \cos 2\beta - (N_{k3}N_{l4} + N_{k4}N_{l3}) \sin 2\beta \right), \quad (\text{A.13})$$

with the real rotation matrix N which diagonalizes the neutralino mass matrix [21], ($k, l = 1, \dots, 4$). One has: $\tilde{\chi}_k^0 = N_{kl} \tilde{\psi}_{Nl}^0$, where $\tilde{\psi}_{Nl}^0 = (-i\tilde{\lambda}_\gamma, -i\tilde{\lambda}_Z, \tilde{\psi}_{H_a}^0, \tilde{\psi}_{H_b}^0)$.

The chargino/neutralino–sfermion–fermion couplings are given in $\mathcal{O}(h_t, h_b, h_\tau)$. The coupling matrices $l_{ij}^{\tilde{f}}$ and $k_{ij}^{\tilde{f}}$ are

$$\begin{aligned} l_{ij}^{\tilde{t}} &= h_t V_{j2} R_{i2}^{\tilde{t}}, & l_{ij}^{\tilde{b}} &= h_b U_{j2} R_{i2}^{\tilde{b}}, \\ k_{ij}^{\tilde{t}} &= h_b U_{j2} R_{i1}^{\tilde{t}}, & k_{ij}^{\tilde{b}} &= h_t V_{j2} R_{i1}^{\tilde{b}}, \end{aligned} \quad (\text{A.14})$$

($i, j = 1, 2$) and as $h_{\nu_\tau} = 0$

$$\begin{aligned} l_{ij}^{\tilde{\nu}_\tau} &= 0, & l_{ij}^{\tilde{\tau}} &= h_\tau U_{j2} R_{i2}^{\tilde{\tau}}, \\ k_{ij}^{\tilde{\nu}_\tau} &= h_\tau U_{j2} R_{i1}^{\tilde{\tau}}, & k_{ij}^{\tilde{\tau}} &= 0. \end{aligned} \quad (\text{A.15})$$

The couplings $\hat{a}_{ik}^{\tilde{f}}$ and $\hat{b}_{ik}^{\tilde{f}}$ are ($i, j = 1, 2$)

$$\hat{a}_{ik}^{\tilde{f}} = h_f R_{i2}^{\tilde{f}} N_k^f, \quad \hat{b}_{ik}^{\tilde{f}} = h_f R_{i1}^{\tilde{f}} N_k^f. \quad (\text{A.16})$$

$k = 1, \dots, 4$ refers to $\tilde{\chi}_k^0$, N_k^f is different for up–type and down–type fermions,

$$\begin{aligned} N_k^t &= N_{k3} \sin \beta - N_{k4} \cos \beta, \\ N_k^{b,\tau} &= -N_{k3} \cos \beta - N_{k4} \sin \beta. \end{aligned} \quad (\text{A.17})$$

References

- [1] H. P. Nilles, *Phys. Rep.* **110** (1984) 1;
A. B. Lahanas and D. V. Nanopoulos, *Phys. Rep.* **145** (1987) 1;
R. Barbieri, *Riv. Nuovo Cimento* **11** (1988) 1.
- [2] H. E. Haber and G. L. Kane, *Phys. Rep.* **117** (1985) 75.
- [3] J. F. Gunion, H. E. Haber, *Nucl. Phys.* **B 272** (1986) 1.
- [4] A. Arhrib, M. Capdequi–Peyranere, A. Djouadi, *Phys. Rev.* **D 52** (1995) 1404.
- [5] H. Eberl, A. Bartl, W. Majerotto, *Nucl. Phys.* **B 472** (1996) 481.
- [6] W. Beenakker, R. Höpker, and P. M. Zerwas, *Phys. Lett.* **B 349** (1995) 463;
S. Kraml, H. Eberl, A. Bartl, W. Majerotto, and W. Porod,
Phys. Lett. **B 386** (1996) 175;
A. Djouadi, W. Hollik, and C. Jünger, *Phys. Rev.* **D 55** (1997) 6975.
- [7] W. Beenakker, R. Höpker und P. M. Zerwas, *Phys. Lett.* **B 378** (1996) 159;
W. Beenakker, R. Höpker, T. Plehn, and P. M. Zerwas, *Z. Physik* **C 75** (1997) 349.
- [8] A. Bartl, H. Eberl, K. Hidaka, S. Kraml, W. Majerotto, W. Porod, and Y. Yamada,
Phys. Lett. **B 389** (1996) 538.

- [9] A. Arhrib, A. Djouadi, W. Hollik, and C. Jünger, *Phys. Rev.* **D 57** (1998) 5860.
- [10] A. Bartl, H. Eberl, K. Hidaka, S. Kraml, W. Majerotto, W. Porod, and Y. Yamada, to be publ. in *Phys. Rev. D*.
- [11] A. Bartl, H. Eberl, K. Hidaka, T. Kon, W. Majerotto, and Y. Yamada, *Phys. Lett.* **B 402** (1997) 303.
- [12] W. Beenakker, R. Höpker, M. Spira, and P. M. Zerwas, *Phys. Rev. Lett.* **74** (1995) 2905, *Z. Physik C* **69** (1995) 163, *Nucl. Phys.* **B 492** (1997) 51.
- [13] M. A. Diaz, S. F. King, and D. A. Ross, *Nucl. Phys.* **B 529** (1998) 23.
- [14] S. Kiyoura, M. M. Nojiri, D. M. Pierce, and Y. Yamada, *Phys. Rev.* **D 58** (1998) 75002.
- [15] J. Guasch, J. Solà, and W. Hollik *Phys. Lett.* **B 437** (1998) 88.
- [16] A. Akeroyd, A. Arhrib, and E. Naimi, hep-ph/9811431.
- [17] H. Eberl, *Thesis*, University of Technology, Vienna, 1998.
- [18] G. 't Hooft and M. Veltman, *Nucl. Phys.* B153 (1979) 365.
- [19] A. Denner, *Fortschr. Phys.* **41** (1993) 307.
- [20] A. Bartl, H. Fraas, W. Majerotto, and B. Möblacher, *Z. Physik C* **55** (1992) 257.
- [21] A. Bartl, H. Fraas, and W. Majerotto, *Nucl. Phys.* **B 278** (1986) 1.
- [22] J. Ellis, G. Ridolfi and F. Zwirner, *Phys. Lett.* **B 262** (1991) 477.
- [23] A. Brignole, *Phys. Lett.* **B 277** (1992) 313.
- [24] E. Lancon (ALEPH), V. Ruhlmann-Kleider (DELPHI), R. Clare (L3) and D. Plane (OPAL), talks at the 50th CERN LEPC meeting, 12 Nov. 1998; for minutes and transparencies, see <http://www.cern.ch/Committees/LEPC/minutes/LEPC50.html>
- [25] DØ Collab., S. Abachi et al., *Phys. Rev. Lett.* **76** (1996) 2222; hep-ph/9902013; CDF Collab., F. Abe et al., *Phys. Rev.* **D 56** (1997) 1357; J. A. Valls, talk at the XXIX International Conference on High Energy Physics (ICHEP98), Vancouver, Canada, 23–29 July 1998, FERMILAB-Conf-98-292-E.
- [26] G. Altarelli, R. Barbieri and F. Caravaglios, *Int. J. Mod. Phys.* **A13** (1998) 1031.
- [27] M. Drees and K. Hagiwara, *Phys. Rev.* **D 42** (1990) 1709.
- [28] J. P. Derendinger and C. A. Savoy, *Nucl. Phys.* **B 237** (1984) 307.

M	$= 200,$	μ	$= 1000,$	$\tan \beta$	$= 4,$	m_A	$= 300,$
$M_{\tilde{Q}}$	$= 225,$	$M_{\tilde{U}}$	$= 200,$	$M_{\tilde{D}}$	$= 250,$	$A_{t,b}$	$= 400.$
$m_{\tilde{t}_1}$	$= 218,$	$m_{\tilde{t}_2}$	$= 317,$	$\cos \theta_{\tilde{t}}$	$= -0.64,$		
$m_{\tilde{b}_1}$	$= 200,$	$m_{\tilde{b}_2}$	$= 278,$	$\cos \theta_{\tilde{b}}$	$= 0.79,$		
$m_{\tilde{\chi}_1^+}$	$= 196,$	$m_{\tilde{\chi}_2^+}$	$= 1007,$	$m_{\tilde{g}}$	$= 559,$		
$m_{\tilde{\chi}_1^0}$	$= 100,$	$m_{\tilde{\chi}_2^0}$	$= 196,$	$m_{\tilde{\chi}_3^0}$	$= 1002,$	$m_{\tilde{\chi}_4^0}$	$= 1007,$
m_{h^0}	$= 93,$	m_{H^0}	$= 305,$	m_{H^+}	$= 298,$	$\sin \alpha$	$= -0.32.$

Table 3: Gaugino scenario, all masses in [GeV].

M	$= 1000,$	μ	$= 200,$	$\tan \beta$	$= 4,$	m_A	$= 300,$
$M_{\tilde{Q}}$	$= 225,$	$M_{\tilde{U}}$	$= 200,$	$M_{\tilde{D}}$	$= 250,$	$A_{t,b}$	$= 400.$
$m_{\tilde{t}_1}$	$= 113,$	$m_{\tilde{t}_2}$	$= 368,$	$\cos \theta_{\tilde{t}}$	$= -0.68,$		
$m_{\tilde{b}_1}$	$= 231,$	$m_{\tilde{b}_2}$	$= 252,$	$\cos \theta_{\tilde{b}}$	$= 0.98,$		
$m_{\tilde{\chi}_1^+}$	$= 196,$	$m_{\tilde{\chi}_2^+}$	$= 1007,$	$m_{\tilde{g}}$	$= 2393,$		
$m_{\tilde{\chi}_1^0}$	$= 190,$	$m_{\tilde{\chi}_2^0}$	$= 202,$	$m_{\tilde{\chi}_3^0}$	$= 509,$	$m_{\tilde{\chi}_4^0}$	$= 1007,$
m_{h^0}	$= 106,$	m_{H^0}	$= 305,$	m_{H^+}	$= 309,$	$\sin \alpha$	$= -0.31.$

Table 4: Higgsino scenario, all masses in [GeV].

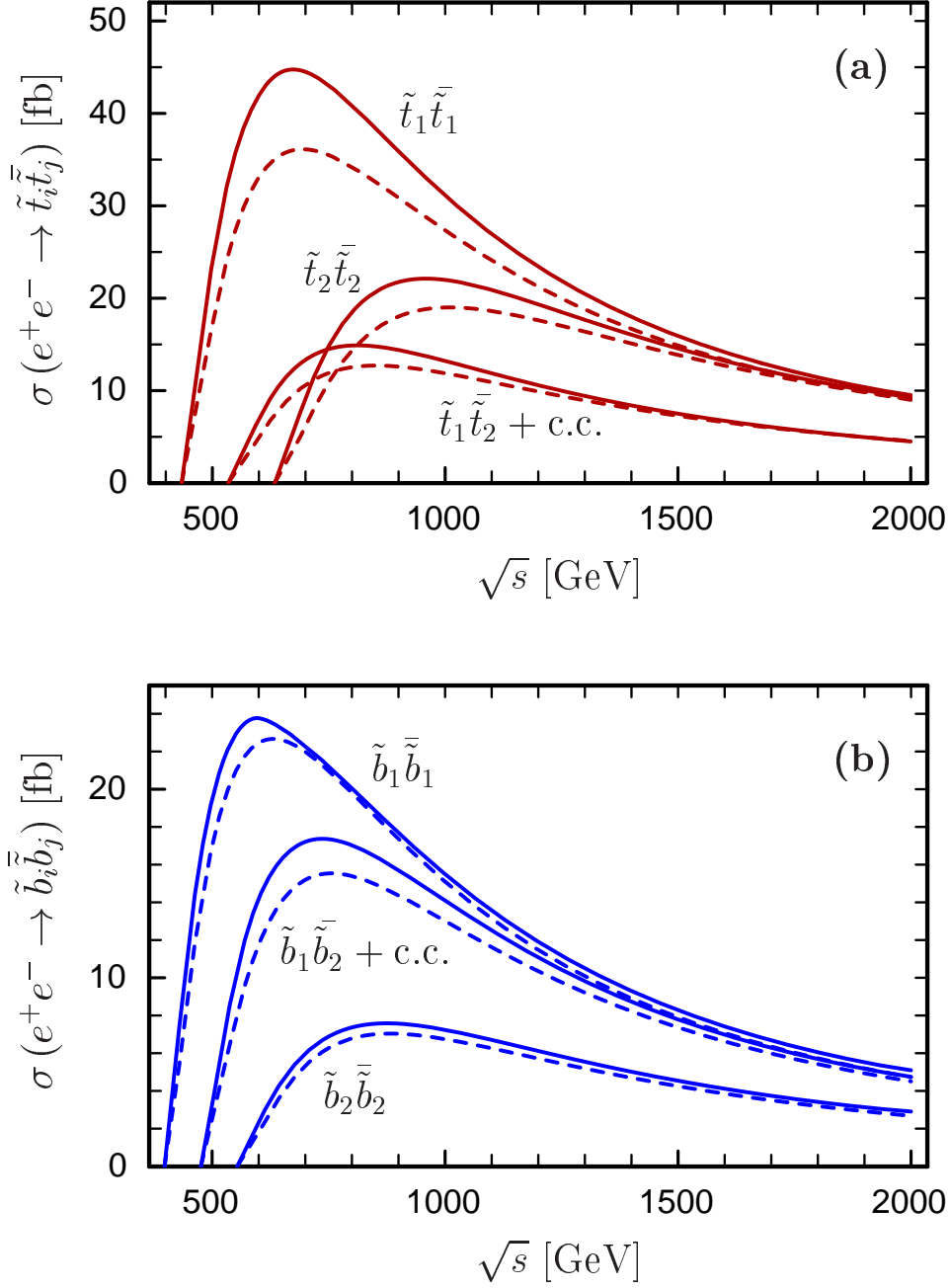


Figure 2: Total (SUSY-QCD and Yukawa coupling) corrected cross sections (full lines) together with the tree-level cross sections (dashed lines) of (a) $e^+e^- \rightarrow \tilde{t}_i \tilde{t}_j$ and (b) $e^+e^- \rightarrow \tilde{b}_i \tilde{b}_j$ for the scenario of Table 3.

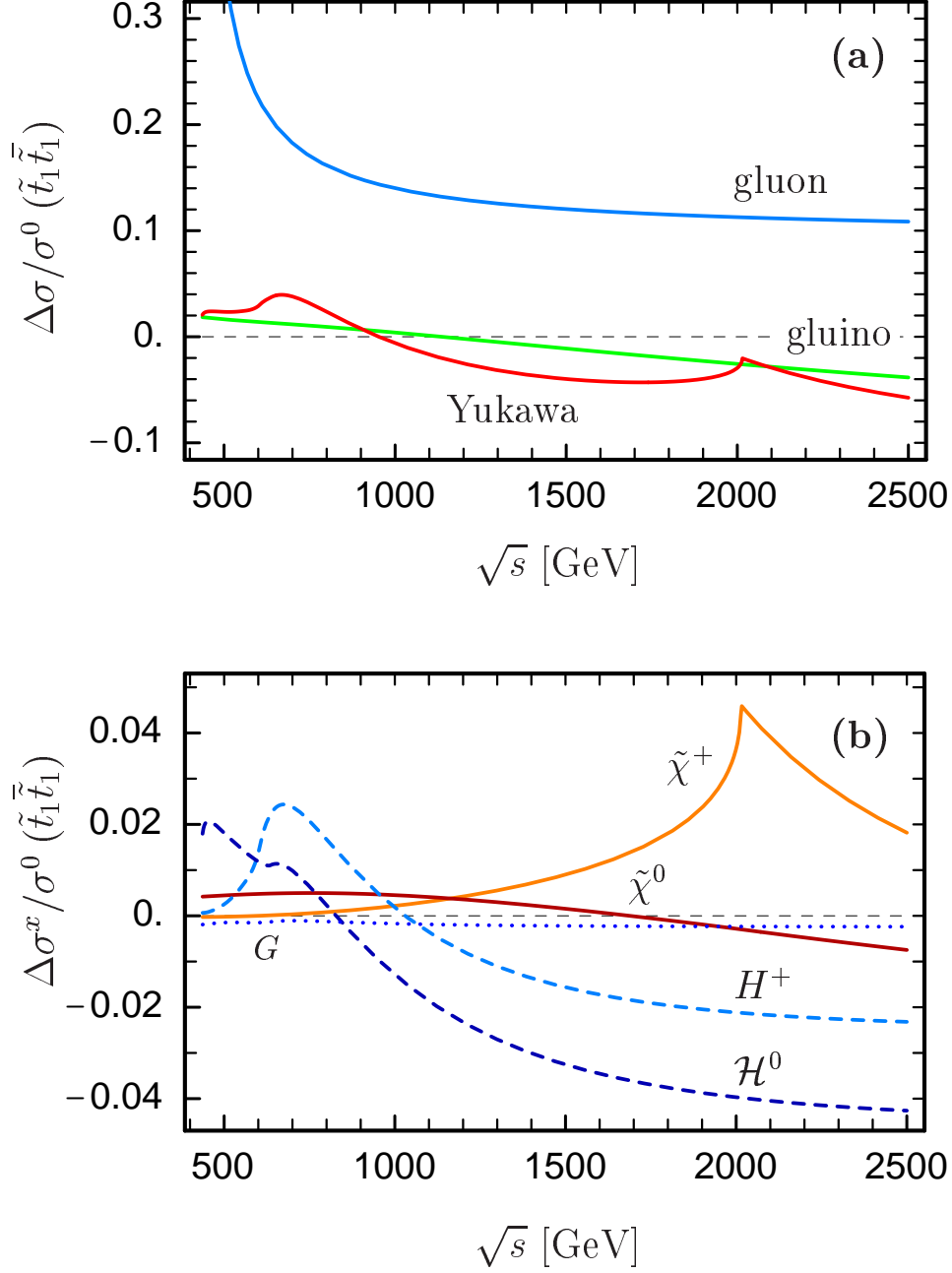


Figure 3: Radiative corrections to $e^+e^- \rightarrow \tilde{t}_1 \tilde{t}_1^*$ relative to the tree-level cross section for the scenario of Table 3: (a) gluon, gluino, and Yukawa coupling corrections and (b) various Yukawa coupling correction contributions.

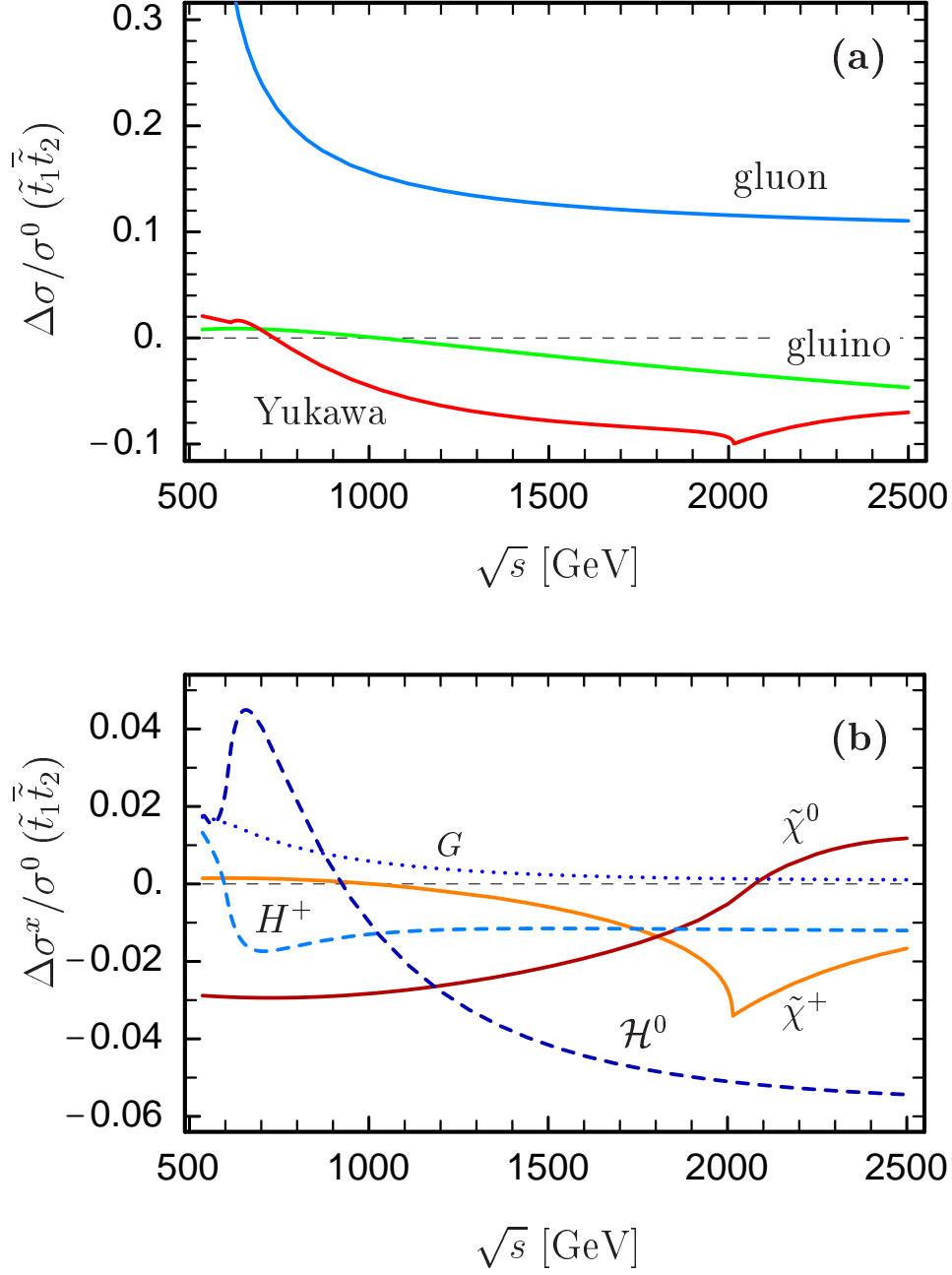


Figure 4: Radiative corrections to $e^+e^- \rightarrow \tilde{t}_1\tilde{t}_2 + \text{c.c.}$ relative to the tree-level cross section for the scenario of Table 3: (a) gluon, gluino, and Yukawa coupling corrections and (b) various Yukawa coupling correction contributions.

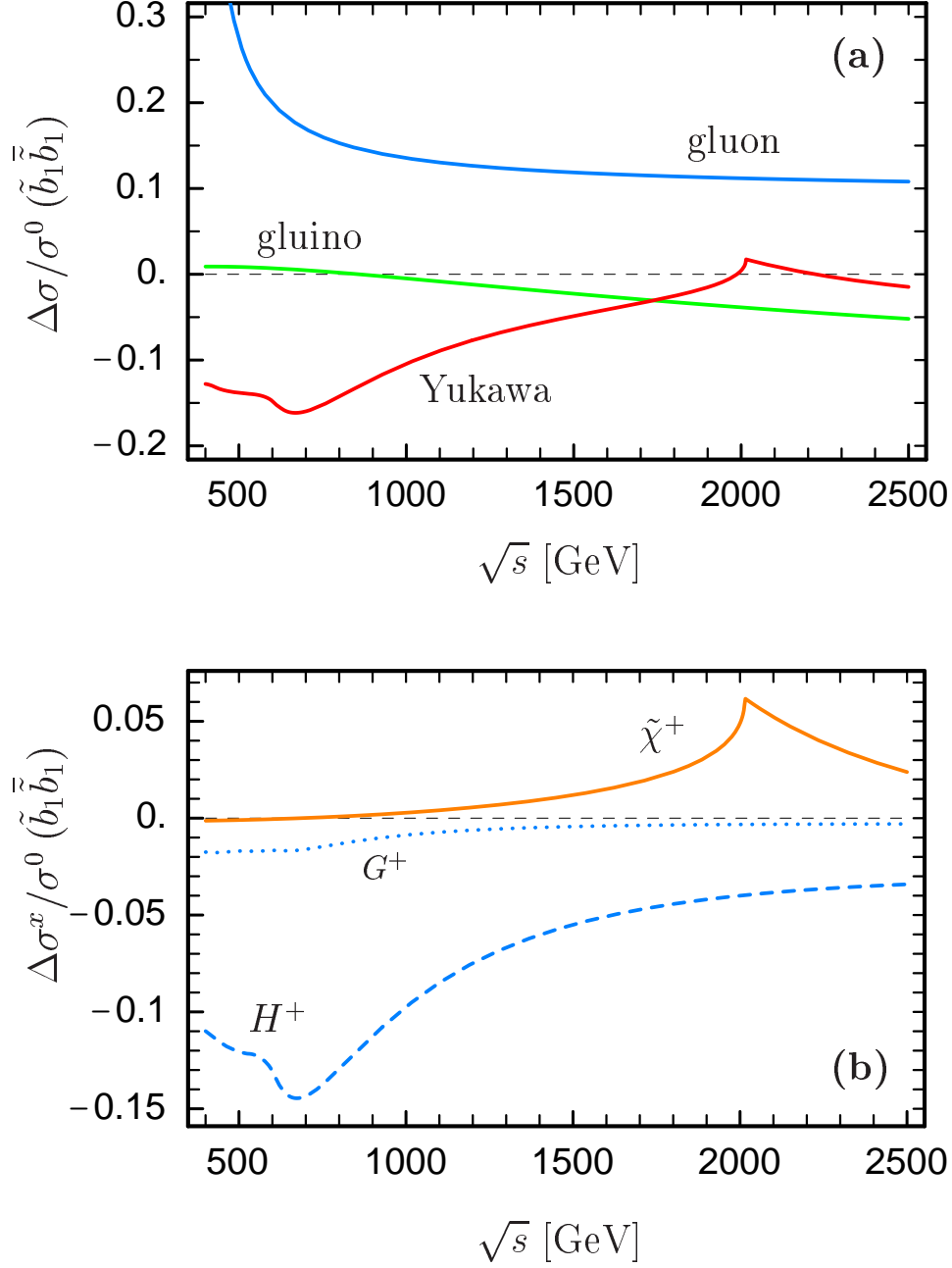


Figure 5: Radiative corrections to $e^+e^- \rightarrow \tilde{b}_1\tilde{b}_1$ relative to the tree-level cross section for the scenario of Table 3: (a) gluon, gluino, and Yukawa coupling corrections and (b) various Yukawa coupling correction contributions.

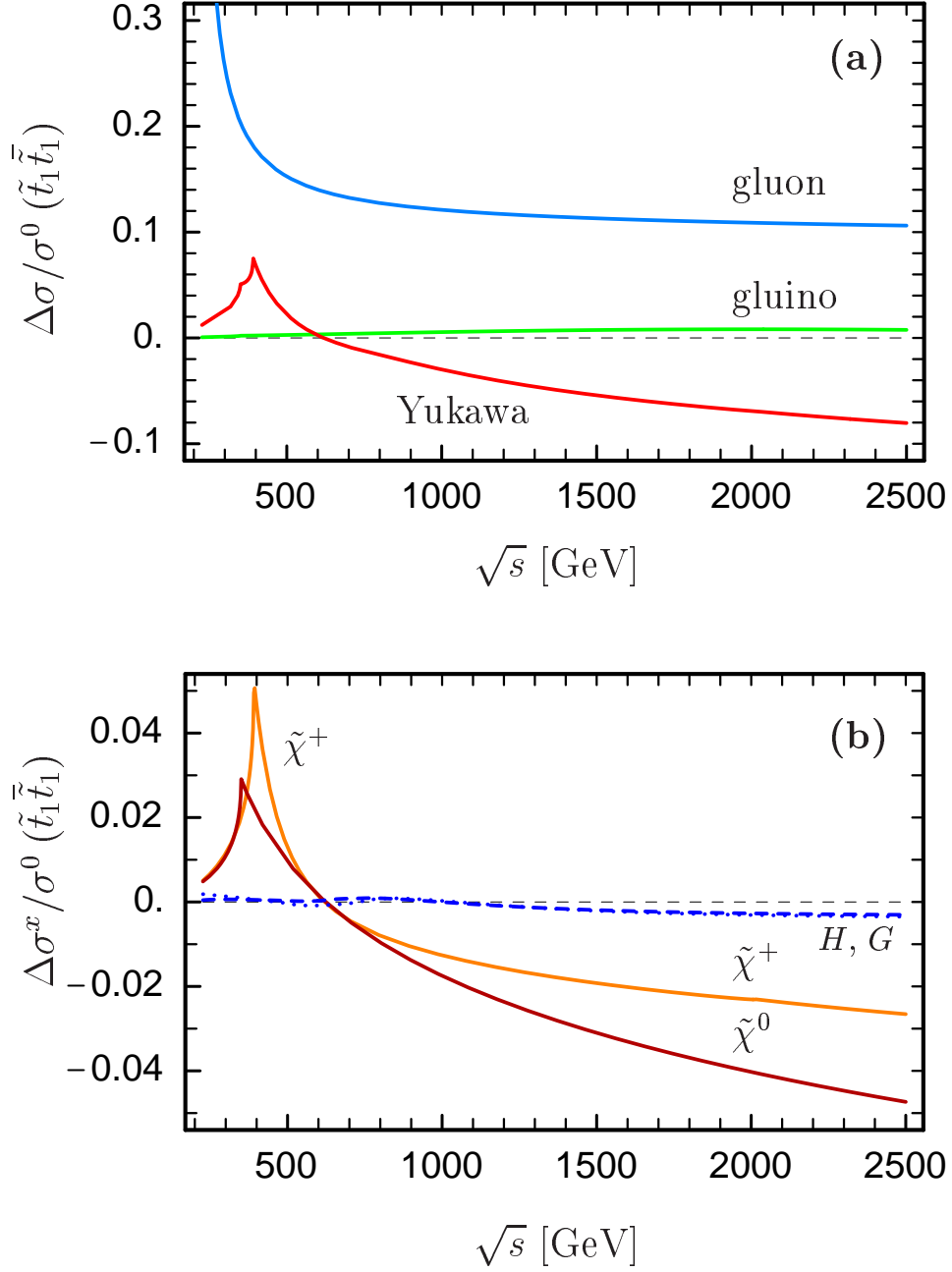


Figure 6: Radiative corrections to $e^+e^- \rightarrow \tilde{t}_1\tilde{t}_1$ relative to the tree-level cross section for the scenario of Table 4: (a) gluon, gluino, and Yukawa coupling corrections and (b) various Yukawa coupling correction contributions.

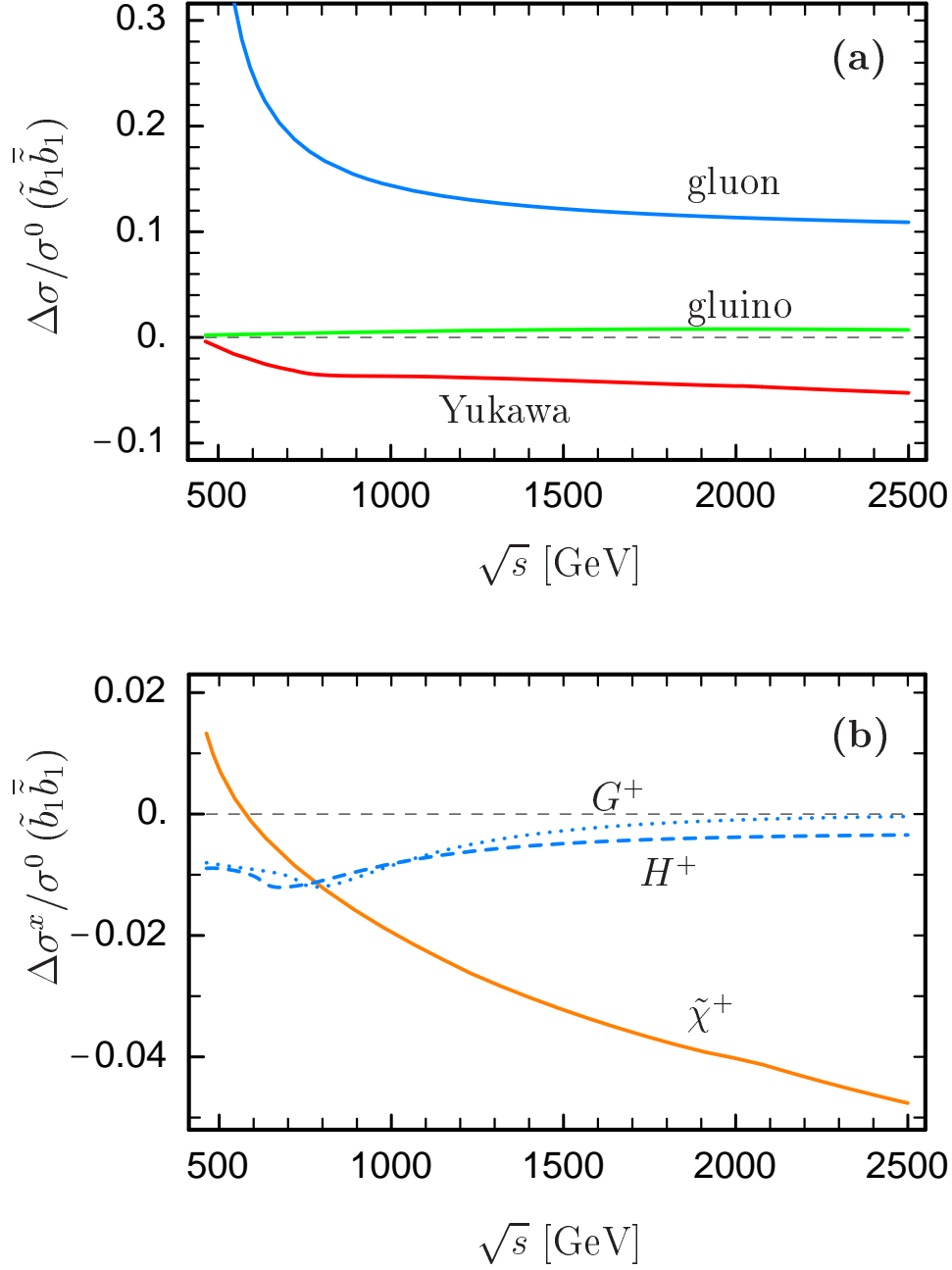


Figure 7: Radiative corrections to $e^+e^- \rightarrow \tilde{b}_1\tilde{b}_1$ relative to the tree-level cross section for the scenario of Table 4: (a) gluon, gluino, and Yukawa coupling corrections and (b) various Yukawa coupling correction contributions.

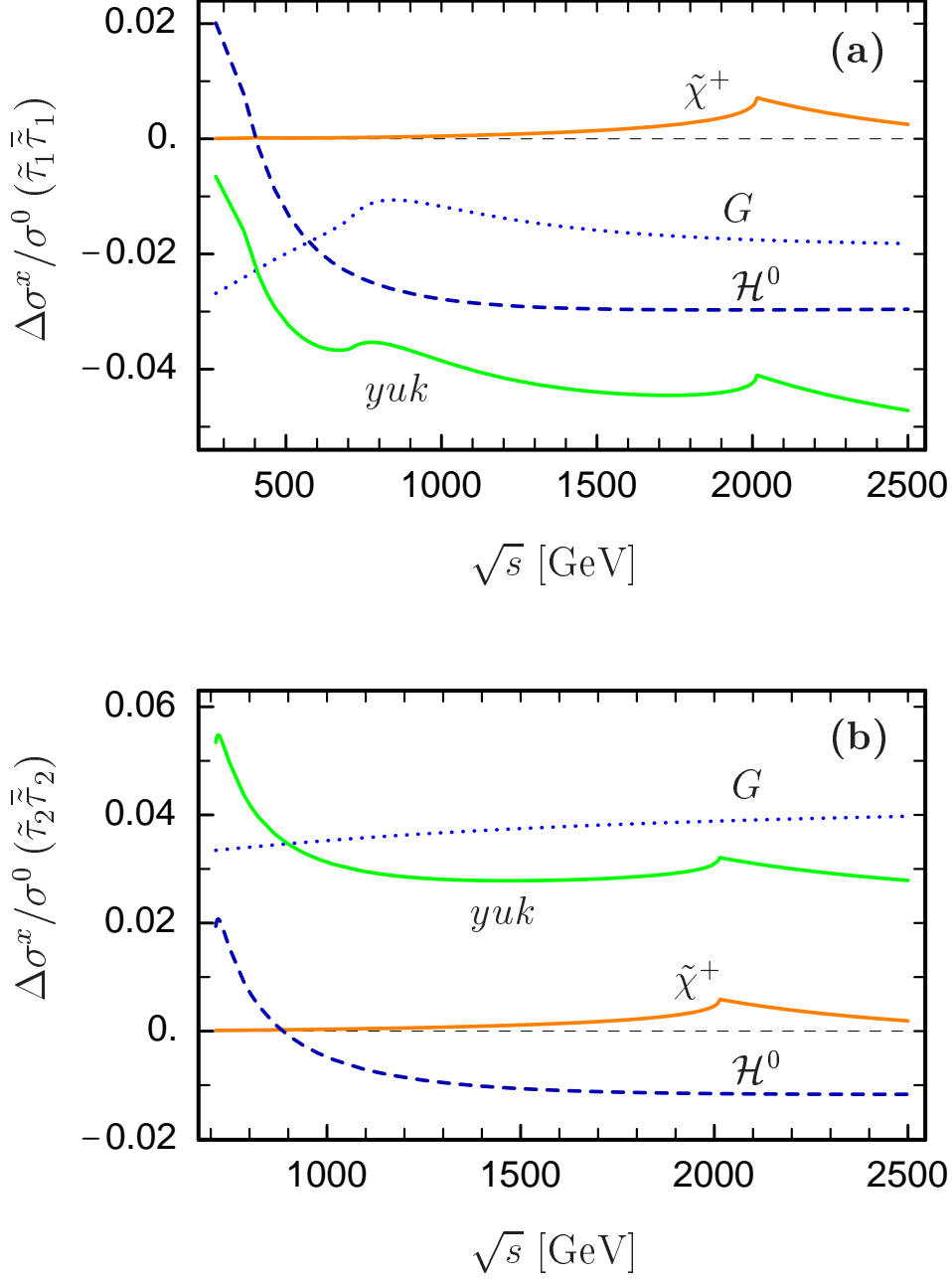


Figure 8: Yukawa coupling correction contributions relative to the tree-level cross section of (a) $e^+e^- \rightarrow \tilde{\tau}_1\bar{\tilde{\tau}}_1$ and (b) $e^+e^- \rightarrow \tilde{\tau}_2\bar{\tilde{\tau}}_2$ for $M_{\tilde{L}} = 280$ GeV, $M_{\tilde{E}} = 250$ GeV, $A_\tau = 100$ GeV, $M = 200$ GeV, $\mu = 1000$ GeV, $\tan\beta = 30$, $m_A = 300$ GeV.